J. Fluid Mech. (1989), *vol.* 202, *pp.* 559–575
Printed in Great Britain

Three-dimensional marginal separation

By P. W. DUCK
Department of Mathematics, University of Manchester, Manchester M13 9PL, UK

(Received 30 June 1988)

The three-dimensional marginal separation of a boundary layer along a line of symmetry is considered. The key equation governing the displacement function is derived, and found to be a nonlinear integral equation in two space variables. This is solved iteratively using a pseudospectral approach, based partly in double Fourier space, and partly in physical space. Qualitatively the results are similar to previously reported two-dimensional results (which are also computed to test the accuracy of the numerical scheme); however quantitatively the three-dimensional results are much different.

1. Introduction

High-Reynolds-number flows may be broadly categorized into two classes, namely attached and detached. The former class generally involves the confinement of a viscous (i.e. boundary) layer to the immediate vicinity of the flow boundary, the flow elsewhere being generally inviscid. A classical example of this is the Blasius flow over a semi-infinite flat plate. The detached class involves viscous layers occurring in the main body of the fluid (as well as on the flow boundaries). An important example of a flow of this class is that of the steady flow past a circular cylinder. This problem has been investigated numerically (for finite Reynolds numbers) by Fornberg (1980, 1985) and models for asymptotically large-Reynolds-number situations been described by Smith (1979, 1985) and by Peregrine (1985), although the precise details of the ultimate high-Reynolds-number flow in this (and similar important cases) are still open to speculation. Generally, attached flows may be thought of as being associated with streamlined bodies, whilst detached flows are more likely to be associated with bluff bodies.

One reason for the great theoretical difficulty in describing detached flows is that generally there appears to be no continuous transition from the fully attached to the grossly detached state. A classical example of this is the work of Goldstein (1948), who showed convincingly, for the first time, how a boundary layer with an adverse pressure gradient would terminate in a singularity right at the point of separation. Some years later Stewartson (1970) showed that this singularity could *not* be removed or alleviated with the inclusion of a triple deck.

The problem studied by Stewartson, Smith & Kaups (1982) (hereafter referred to as I) was that of two-dimensional marginal separation. Here the question was the behaviour of a boundary layer that is on the verge of separating at a point, but then recovers. This work showed how an interaction region was formed, centred at the point of zero wall shear, which served to smooth out the discontinuous streamwise gradient of the shear stress at this point. Further, it was shown in I (by the solution of a nonlinear integral equation) that by means of varying an arbitrary parameter (Γ in their notation) that: (i) separated flow was possible within the interaction zone;

(ii) for certain values of Γ the solution exhibited non-uniqueness; (iii) there exists a critical value of Γ above which no solution exists. (This latter conclusion is a further example of a lack of uniform transition from a fully attached to a grossly detached state.) A thorough investigation of the aforementioned integral equation was mounted by Brown & Stewartson (1983), and this revealed that up to four solutions were possible for certain values of the parameter Γ.

One of the motivations for this work was a numerical investigation of laminar boundary layers on smooth bodies of revolution at incidence, carried out by Cebeci, Khattab & Stewartson (1980). In this study, the classical boundary-layer equations along the line of symmetry were integrated numerically, and it was found that at one particular angle of incidence (40° for the case cited), the skin friction dipped (linearly) to zero at one location, and then rose quickly again. At a very slightly increased angle of incidence (41°) the separation process turns out to be catastrophic (although this is not unexpected, owing to the non-interacting nature of the calculation). More recently, Cebeci & Su (1988) have considered the full three-dimensional boundary-layer problem on a prolate spheroid, focusing much attention on the separation aspect. Smith (1982) considered the unsteady counterpart of the problem considered in I, and found that a finite-time breakdown of the solution was possible, which he attributed to the occurrence of dynamic stall.

In an attempt to model the Cebeci *et al.* (1980) configuration rather better, Brown (1985) (hereafter referred to as II) considered the problem of marginal separation of a boundary layer along a line of symmetry. The result of the analysis was again an integral equation, although this time two constants were found necessary (although these turn out to be related). One important assumption with that work is an *a priori* knowledge of the crossflow pressure gradient (obtained from inviscid theory), and so that work may be described as mildly three-dimensional, although it does have interesting and important differences from the two-dimensional work of I. In particular, in general the upstream streamwise gradient of skin friction is no longer minus the downstream gradient (the ratio of these quantities being a parameter of the problem).

The aim of this paper is to treat a fully three-dimensional marginal separation (again along a line of symmetry), incorporating crossflow pressure variations in the interaction zone. Following I and II we assume that the boundary layer has a particular form at the separation point, which lies on the line of symmetry. Defining the streamwise direction to be parallel to the line of symmetry, and the crossflow direction perpendicular to the line of symmetry, we then make a key assumption (akin to that used in I and II), that the streamwise component of skin friction vanishes simultaneously (at the separation point) with the crossflow derivative of the crossflow component of skin friction. The precise details will be described in the following section.

Work on three-dimensional interacting boundary layers (a category to which this work relates) has progressed somewhat slowly. Smith, Sykes & Brighton (1977) posed the three-dimensional triple-deck problem, which they then solved for a linearized case. Duck & Burggraf (1986) used a pseudospectral method to treat the fully nonlinear version of Smith *et al.* (1977), and obtained solutions for a number of separated flows. Smith (1983) (extended by Bodonyi & Duck 1988) presented a finite-difference scheme for treating flows of this type, using a system of rotated coordinates, enabling the problem to be made quasi-two-dimensional. The amount of literature on three-dimensional separation remains small, in spite of its great importance; this would appear to be due to the great numerical difficulties

encountered with flows of this type. Indeed the author is unaware of any detailed studies of the three-dimensional Goldstein singularity *per se* (although Cebeci *et al.* 1980 do have some discussion of this point).

The outcome of the analysis of this paper is a two-dimensional nonlinear integral equation (or partial integro–differential equation depending on the final form used). (The work of I and II resulted in an analogous one-dimensional equation.) In order to solve this equation, we shall adopt a pseudospectral approach, with the solution technique being based partly in Fourier space, and partly in physical space. This type of approach is in the spirit of Duck & Burggraf (1986), although the details are very much different. It appears that this type of approach has considerable advantages over solution procedures confined to physical variables.

2. Basic formulation

Let us consider an incompressible fluid of kinematic viscosity ν. Suppose that L denotes a typical lengthscale in the problem (for example the distance between a leading edge/stagnation point and the separation point), and that a typical free-stream velocity directed along the centreline is U_∞. Then we take Cartesian coordinates (Lx, Ly, Lz), with the origin at the separation point; the flow velocity is $U_\infty \boldsymbol{u} = U_\infty(u, v, w)$, and we define the centreline to lie along $z = 0$. The body surface (ignoring any curvature terms) lies on the plane $y = 0$. The pressure is written as $\rho U_\infty^2 p$, where ρ is the fluid density. The Reynolds number (assumed large throughout this paper) is defined as

$$R = U_\infty L/\nu. \tag{2.1}$$

The governing non-dimensional equations are then written as

$$\boldsymbol{\nabla}\cdot\boldsymbol{u} = 0, \tag{2.2}$$

$$(\boldsymbol{u}\cdot\boldsymbol{\nabla})\,\boldsymbol{u} = -\boldsymbol{\nabla}p + R^{-1}\,\boldsymbol{\nabla}^2\boldsymbol{u}. \tag{2.3}$$

We shall suppose that all three velocity components are (generally) non-zero and functions of x, y, z. Because of the symmetry of the problem about $z = 0$, we expect u, v and p to be even functions about the centreline, whilst w will be an odd function of z.

Finally, on $y = 0$ we need to impose the usual conditions of zero velocity, i.e.

$$\boldsymbol{u} = 0 \quad \text{on} \quad y = 0. \tag{2.4}$$

3. Non-interacting flow

As the flow approaches the point of zero skin friction ($x = y = z = 0$) we suppose that the boundary layer has the standard thickness $O(R^{-\frac{1}{2}})$. However, rather than allowing the boundary layer at this point to have a Goldstein (1948) 'square-root' singularity, we assume that ambient conditions are such that this is avoided. This we achieve (following I and II) by a careful choice of conditions (as defined in (3.11) below), which results in the boundary layer exhibiting a streamwise gradient of streamwise wall shear (and crossflow derivative of streamwise gradient of crossflow wall shear) that is discontinuous at $x = z = 0$. We now seek to determine the general

form of this solution under these conditions, in this region. Taking (2.2), (2.3) and introducing classical boundary-layer variables,

$$y = R^{-\frac{1}{2}}Y, \tag{3.1}$$

$$v = R^{-\frac{1}{2}}V, \tag{3.2}$$

with all other variables (both dependent and independent) remaining unchanged, then the three-dimensional boundary-layer equations can be written (to leading order)

$$\frac{\partial u}{\partial x}+\frac{\partial V}{\partial Y}+\frac{\partial w}{\partial z}=0, \tag{3.3}$$

$$u\frac{\partial u}{\partial x}+V\frac{\partial u}{\partial Y}+w\frac{\partial u}{\partial z}=-\frac{\partial p}{\partial x}+\frac{\partial^2 u}{\partial Y^2}, \tag{3.4}$$

$$u\frac{\partial w}{\partial x}+V\frac{\partial w}{\partial Y}+w\frac{\partial w}{\partial z}=-\frac{\partial p}{\partial z}+\frac{\partial^2 w}{\partial Y^2}, \tag{3.5}$$

$$\frac{\partial p}{\partial Y}=0. \tag{3.6}$$

We now *assume* the following solution expansions (in line with our earlier remarks):

$$\begin{aligned} u = {} & U_0(Y)+\mu(\lambda^2x^2+z^2)^{\frac{1}{2}}U_0'(Y) \\ & -x[w_1(Y)+V_1'(Y)]+\tfrac{1}{2}x^2[-V_2'(Y)-w_2(Y)] \\ & +\tfrac{1}{2}\mu^2(\lambda^2x^2+z^2)\,U_0''(Y)+z^2u_{23}(Y) \\ & -\mu x(\lambda^2x^2+z^2)^{\frac{1}{2}}(V_1''+w_1')+\ldots, \end{aligned} \tag{3.7}$$

$$\begin{aligned} V = {} & V_1(Y)-\frac{\mu\lambda^2x}{(\lambda^2x^2+z^2)^{\frac{1}{2}}}U_0(Y)+xV_2(Y) \\ & -\mu^2\lambda^2xU_0'-\mu(\lambda^2x^2+z^2)^{\frac{1}{2}}(w_1(Y)-V_1'(Y)) \\ & +\frac{x^2\lambda^2\mu}{(\lambda^2x^2+z^2)^{\frac{1}{2}}}(2w_1+V_1')+\ldots, \end{aligned} \tag{3.8}$$

$$w = zw_1(Y)+xzw_2(Y)+\mu z(\lambda^2x^2+z^2)^{\frac{1}{2}}w_1'(Y)+\ldots, \tag{3.9}$$

$$P = P_0+P_1x+\tfrac{1}{2}P_2x^2+\tfrac{1}{2}P_3z^2+\ldots. \tag{3.10}$$

The key assumption here is that the solution is generally non-differentiable in a small elliptic region centred about $x = z = 0$. The parameter μ is essentially a lengthscale parameter, whilst λ is a measure of the aspect ratio of the elliptic region (which may also be related to the relative magnitude of the streamwise and cross flow velocities, close to the surface). Notice that (3.7)–(3.10) satisfy the continuity equation (3.3).

In order that the appropriate boundary conditions on $y = 0$ are satisfied, we must have

$$U_0(0) = U_0' = 0, \quad V_1(0) = V_1'(0) = 0, \tag{3.11a, b}$$

$$w_1(0) = w_1'(0) = 0 \quad \text{(and hence } V_1'' = 0\text{)}, \qquad w_2(0) = V_2(0) = 0, \tag{3.11c, d}$$

$$V_2'(0) = \mu^2\lambda^2U_0''(0), \quad u_{23}(0) = -\tfrac{1}{2}\mu^2U_0''(0). \tag{3.11e, f}$$

The key assumptions here, at least from the physical point of view, are (3.11*a*, *c*) (the remainder of these conditions are basically zero-velocity restraints). Equation (3.11*a*) demands that at $x = z = 0$ the streamwise component of wall shear vanishes (cf. I and II), whilst (3.11*c*) demands that the z-derivative of crossflow wall shear vanishes, simultaneously, at this point.

Since we expect the solution to be regular as $Y \to 0$, we may expand the solution in the form of a Taylor series in this limit, for example

$$U_0(Y) = \sum_{n=2}^{\infty} \frac{a_n Y^n}{n!}, \tag{3.12}$$

$$w_1(Y) = \sum_{n=2}^{\infty} \frac{c_n Y^n}{n!}. \tag{3.13}$$

It is a simple matter to show that

$$V_1(Y) = -U_0 \int_0^Y \frac{U_0 w_1 - P_1 + U_0''}{U_0^2} \mathrm{d}Y. \tag{3.14}$$

However we expect V_1 to be regular as $Y \to 0$ also, and this condition then also demands

$$\left.\begin{aligned} a_2 = U_0''(0) = P_1, \quad a_3 = U_0'''(0) = 0, \\ a_4 = U_0^{(\mathrm{iv})}(0) = 0, \quad U_0^{(\mathrm{v})}(0) = a_3 = 0. \end{aligned}\right\} \tag{3.15}$$

A similar, local analysis with the z-momentum equation, as $Y \to 0$, reveals the solution to remain regular provided the following additional conditions are fulfilled:

$$c_2 = w_1''(0) = P_3, \quad c_3 = 0, \quad c_4 = w_1^{(\mathrm{iv})}(0) = c_2^2. \tag{3.16}$$

(A similar analysis is also possible with V_2 and w_2, although we have more than enough details to proceed to the next stage of the analysis.)

At this stage it is interesting to distinguish between the above, I and II. Setting $z = 0, w_1 = w_2 = \ldots = 0$, together with $\mu = 1$ in the above, reduces the system to one identical to that described in I. The key difference from the work of II is that, in the latter, no restriction was placed on $w_1'(0)$; the primary repercussion of this was that, unlike the above (and I), the no-slip condition downstream ($x > 0$) was violated, and so an inner Goldstein-type layer was found necessary. This leads to a situation, in general, where the downstream wall shear is no longer symmetrical about $x = 0$ (as is the case in the above and I). A further difference in II was that the discontinuity in wall shear was centred along a line ($x = 0$), (rather than at a point, as above); thus the present structure is rather more three-dimensional. A further important distinction is described later.

It is interesting to note that conditions (3.11*a–c*) imply that at $x = z = 0$ all components of the vorticity vector on the wall are zero, and this is exactly the condition for a point of separation as described by Lighthill (1963). Thus the situation described above is important generically.

Unfortunately, owing to the limited literature available on integrating the three-dimensional boundary-layer equations (even of a non-interacting nature), there do not appear to be any calculations illustrating the above characteristics. (Cebeci *et al.* 1980 did present an example of flow past the special case of a paraboloid of zero thickness, with a point where $U_0'(0) = 0$, but with $w_1'(0) \neq 0$; this provided the stimulus for the work of II.)

The discontinuity in slope at the origin of the solution here (and in I and II) is removed by means of a triple deck, centred at $x = y = z = 0$, and we focus our attention on this aspect next.

4. The interacting region

As in I and II, the appropriate streamwise scale is $x = O(\delta)$, where $\delta = R^{-\frac{1}{5}}$. We also expect the appropriate crossflow lengthscale to be the same, namely $z = O(\delta)$, and so scaled variables (X, Z) are defined by

$$X = x/\delta, \tag{4.1}$$

$$Z = z/\delta. \tag{4.2}$$

Consider first the main deck, comparable in thickness with the classical boundary layer described in the previous section.

The expansion for the solution in this ($Y = O(1)$) region (guided partly by (3.7)–(3.10), and partly by I and II) is

$$\begin{aligned} u = {} & U_0(Y) + \delta\{-X[w_1(Y) + V_1'(Y)] + A(X,Z)\,U_0'(Y)\} + \delta^2\{-\tfrac{1}{2}X^2[V_2'(Y) + w_2(Y)] \\ & + \tfrac{1}{2}[A(X,Z)^2 + \gamma(Z)]\,U_0''(Y) \\ & + Z^2 u_{23}(Y) - XA(X,Z)[V_1''(Y) + w_1'(Y)]\} + \ldots, \end{aligned} \tag{4.3}$$

$$\begin{aligned} V = {} & V_1(Y) = A_X\,U_0(Y) \\ & + \delta\{XV_2(Y) = AA_X\,U_0'(Y) + (XA)_X(V_1'(Y) + w_1(Y)) - (ZA)_Z\,w_1(Y)\} + \ldots \end{aligned} \tag{4.4}$$

$$w = \delta[Zw_1(Y)] + \delta^2\{XZw_2(Y) + ZA(X,Z)\,w_1'(Y)\} + \ldots, \tag{4.5}$$

$$P = P_0 + \delta P_1 X + \tfrac{1}{2}\delta^2 P_2 X^2 + \tfrac{1}{2}\delta^2 P_3 Z^2 + \delta^{\frac{5}{2}}\tilde{P}(X,Z) + \ldots. \tag{4.6}$$

The function $\gamma(Z)$ here is an arbitrary function of Z, which as we shall see performs a key role in the investigation, and is analogous to the constant Γ in I. $\gamma(Z)$ is a function we may postulate, although we shall assume $\gamma = o(Z^2)$ as $Z \to \infty$ in order that a proper match is made with the results of the previous section. The functions $A(X,Z)$ and $\tilde{P}(X,Z)$ are a displacement function and pressure perturbation respectively, and arise from the interaction to be described shortly.

In order that a proper match is made with (3.7)–(3.10) we require

$$A^2(X,Z) \to \mu^2(\lambda^2 X^2 + Z^2) \quad \text{as} \quad X^2 + Z^2 \to \infty. \tag{4.7}$$

The system (4.3)–(4.6) clearly violates the no-slip condition on $Y = 0$, and hence the inclusion of a lower deck is necessary. In order that a meaningful balance of terms is effected, this must have thickness given by

$$\tilde{Y} = Y\delta^{-\frac{1}{4}} = O(1) \tag{4.8}$$

(the same thickness as found in I and II). In this region, the solution expansion given in (4.3)–(4.5) remains essentially unchanged, except that Y is replaced by $\delta^{\frac{1}{4}}\tilde{Y}$, and there is a correction to the u-expansion of $\delta^2\tilde{U}(X,\tilde{Y},Z)$, to the V expansion of $\delta^{\frac{5}{4}}\tilde{V}(X,Y,Z)$ and to the w expansion of $\delta^2\tilde{W}(X,\tilde{Y},Z)$. The governing equations for these correction terms are

$$\frac{\partial\tilde{U}}{\partial X} + \frac{\partial\tilde{V}}{\partial\tilde{Y}} + \frac{\partial\tilde{W}}{\partial Z} = 0, \tag{4.9}$$

$$\tfrac{1}{2}a_2\tilde{Y}^2\frac{\partial\tilde{U}}{\partial X}+a_2\tilde{Y}\tilde{V}=-\frac{\partial\tilde{P}}{\partial X}+\frac{\partial^2\tilde{U}}{\partial\tilde{Y}^2}, \tag{4.10}$$

$$\tfrac{1}{2}a_2\tilde{Y}^2\frac{\partial\tilde{W}}{\partial X}=\frac{\partial^2\tilde{W}}{\partial\tilde{Y}}-\frac{\partial\tilde{P}}{\partial Z}, \tag{4.11}$$

where
$$a_2=U_0''(0). \tag{4.12}$$

The boundary conditions to be applied to this system are that

$$\tilde{U},\tilde{W}\to 0 \quad \text{as} \quad \tilde{Y}\to\infty,$$

together with

$$\left.\begin{aligned}\tilde{W}(\tilde{Y}=0)&=\tilde{V}(\tilde{Y}=0)=0,\\ \tilde{U}(\tilde{Y}=0)&=-\frac{a_2}{2}\{A^2+\gamma(Z)-\mu^2(\lambda^2X^2+Z^2)\}.\end{aligned}\right\} \tag{4.13}$$

Differentiating (4.10) with respect to X, and (4.11) with respect to Z, and adding yields

$$\tfrac{1}{2}a_2\tilde{Y}^2\left(\frac{\partial^2\tilde{U}}{\partial X^2}+\frac{\partial^2\tilde{W}}{\partial X\,\partial Z}\right)+a_2\tilde{Y}\frac{\partial\tilde{V}}{\partial X}=-\frac{\partial^2\tilde{P}}{\partial X^2}-\frac{\partial^2\tilde{P}}{\partial Z^2}+\frac{\partial^3\tilde{U}}{\partial Y^2\,\partial X}+\frac{\partial^3\tilde{W}}{\partial\tilde{Y}^2\,\partial Z}. \tag{4.14}$$

Invoking continuity (4.9), and then differentiating with respect to $\tilde{Y}$ yields

$$\frac{\partial^4\tilde{V}}{\partial\tilde{Y}^4}-\tfrac{1}{2}a_2\tilde{Y}^2\frac{\partial^3\tilde{V}}{\partial\tilde{Y}^2\,\partial X}+a_2\frac{\partial\tilde{V}}{\partial X}=0. \tag{4.15}$$

Here the problem has been reduced to a (quasi-) two-dimensional problem, which greatly simplifies obtaining a solution. The boundary conditions to be imposed are: on $\tilde{Y}=0$

$$\left.\begin{aligned}\tilde{V}&=0,\\ \frac{\partial\tilde{V}}{\partial\tilde{Y}}&=\tfrac{1}{2}a_2[2AA_X-2\mu^2\lambda^2X],\\ \frac{\partial^3\tilde{V}}{\partial\tilde{Y}^3}&=-\frac{\partial^2\tilde{P}}{\partial X^2}-\frac{\partial^2\tilde{P}}{\partial Z^2},\end{aligned}\right\} \tag{4.16}$$

whilst $\tilde{V}\to 0$ as $\tilde{Y}\to\infty$.

A very similar system was considered by Stewartson (1970), the key result of which shows that a solution subject to (4.16) is only possible if

$$\tfrac{1}{2}a_2[A^2+\gamma(Z)-\mu^2(\lambda^2X^2+Z^2)]=-\frac{(-\frac{1}{4}!)}{2^{\frac{3}{2}}(\frac{1}{4}!)}\int_{-\infty}^{X}\frac{\dfrac{\partial\tilde{P}}{\partial\xi}+\displaystyle\int_{-\infty}^{\xi}\frac{\partial^2\tilde{P}}{\partial Z^2}\,\mathrm{d}\xi}{(X-\xi)^{\frac{1}{2}}}\,\mathrm{d}\xi \tag{4.17}$$

(subject to (4.7)).

The system is now closed by consideration of the upper deck, wherein $Y=O(\delta^{-\frac{3}{2}})$. The solution is standard, with the pressure being determined by Laplace's equation, and so, following Smith *et al.* (1977) and Duck & Burggraf (1986), we may write

$$\tilde{P}(X,Z)=-\frac{1}{2\pi}U_0(\infty)^2\int_{-\infty}^{\infty}\int_{-\infty}^{\infty}\frac{\partial^2A/\partial\xi^2\,\mathrm{d}\xi\,\mathrm{d}\zeta}{[(X-\xi)^2+(Z-\zeta)^2]^{\frac{1}{2}}}. \tag{4.18}$$

The combination of (4.17) and (4.18) represents a closed problem, the solution of which will be discussed in the following section.

We note that the condition (4.6) as $X^2+Z^2\to\infty$ can be made stronger, namely

$$A^2(X,Z)\to\mu^2(\lambda^2X^2+Z^2)-\gamma(Z). \tag{4.19}$$

This is analogous to the far-field condition found in I,

$$A^2(X)\sim X^2-\Gamma \tag{4.20}$$

(where Γ is a constant). We note that if $\gamma(Z)$ is entirely negative, then we might expect there to be no difficulty in obtaining a solution to the system described above, with the flow remaining entirely attached. However as $\gamma(Z)$ increases, and becomes progressively more positive, (4.19) suggests that a three-dimensional analogue to the classical Goldstein square-root singularity is possible, leading to a catastrophic breakdown. (Indeed, similar observations are noted in the work of I and II.) One of the primary aims of the following sections will be to determine the maximum value of $\gamma(Z)$ for which solutions exist. Notice, also, that as $\gamma(Z)$ becomes progressively more negative the effect of the interaction is reduced, and (4.19) becomes an asymptotic solution to the above system.

In II it was assumed that the cross-stream pressure gradient was known *a priori* (not a completely rational assumption), leading to a one-dimensional mathematical problem, similar to that found in I; here, the mathematical problem (4.17) and (4.18) is fully two-dimensional.

5. Numerical technique

At this stage it is convenient to take the double Fourier Transform of (4.17) and (4.18) to eliminate the pressure perturbation $\tilde{P}(X,Z)$. Defining

$$A^{**}=\int_{-\infty}^{\infty}\int_{-\infty}^{\infty}A(X,Z)\,\mathrm{e}^{-\mathrm{i}kX-\mathrm{i}lZ}\,\mathrm{d}X\,\mathrm{d}Z \tag{5.1}$$

(with other transform quantities defined similarly), then (4.17) and (4.18) give

$$\tfrac{1}{2}a_2[A^2+\gamma(Z)-\mu(\lambda^2X^2+Z^2)]^{**}=-\frac{(-\frac{1}{4}!)}{2(\frac{1}{4}!)}(\tfrac{1}{2}\pi)^{\frac{1}{2}}(\mathrm{i}k)^{\frac{1}{2}}(k^2+l^2)^{\frac{1}{4}}U_0(\infty)^2A^{**}. \tag{5.2}$$

This equation can be transformed back into (X,Z)-space, giving

$$A(X,Z)=-\Lambda\int_{-\infty}^{\infty}\int_{-\infty}^{\infty}\frac{L(\xi,\zeta)\,K(\chi)}{[(X-\xi)^2+(Z-\zeta)^2]^{\frac{1}{4}}}\,\mathrm{d}\xi\,\mathrm{d}\zeta, \tag{5.3}$$

where $K(\chi)$ denotes the complete elliptic integral of the first kind, argument χ, where

$$\chi=\left[1+\frac{X-\xi}{[(X-\xi)^2+(Z-\zeta)^2]^{\frac{1}{2}}}\right]^{\frac{1}{2}}, \tag{5.4}$$

and

$$L(X,Z)=\tfrac{1}{2}a_2[A^2+\gamma(Z)-\mu^2(\lambda^2X^2+Z^2)] \tag{5.5}$$

and

$$\Lambda=\frac{8(\frac{1}{4}!)}{\pi^{\frac{3}{2}}(-\frac{1}{4}!)\,U_0(\infty)^2}. \tag{5.6}$$

However from a numerical point of view (5.3) would present a number of difficulties, primarily associated with singularities in the kernel term. Instead we

prefer to adopt an alternative scheme based on the transform equation (5.2). If we write

$$(A,\gamma,X,Z,k,l)=(\beta\mu^{\frac{3}{5}}\hat{A},\beta^2\mu^{\frac{6}{5}}\hat{\gamma},\beta\mu^{-\frac{2}{5}}\hat{X},\beta\mu^{-\frac{2}{5}}\hat{Z},\beta^{-1}\mu^{\frac{2}{5}}\hat{k},\beta^{-1}\mu^{\frac{2}{5}}\hat{l}), \tag{5.7}$$

where

$$\beta=\left[\frac{(-\frac{1}{4}!)\,(\frac{1}{2}\pi)^{\frac{1}{2}}}{(\frac{1}{4}!)\,a_2}U_0^2(\infty)\right]^{\frac{2}{5}}, \tag{5.8}$$

then (5.2) simplifies to

$$[\hat{A}^2+\hat{\gamma}(\hat{Z})-(\lambda^2\hat{X}^2+\hat{Z}^2)]^{**}=-(\mathrm{i}\hat{k})^{\frac{1}{2}}(\hat{k}^2+\hat{l}^2)^{\frac{1}{2}}\hat{A}^{**}. \tag{5.9}$$

In its present form (5.9) is unsuitable for numerical manipulations, because of unboundedness as $\hat{X}^2+\hat{Z}^2\to\infty$. (This is mirrored in $(\hat{k},\hat{l})$-space by a singularity as $\hat{k}$ and/or $\hat{l}\to 0$.) We do, however, have the condition

$$\hat{A}^2\sim\lambda^2\hat{X}^2+\hat{Z}^2-\hat{\gamma}(\hat{Z})\quad\text{as}\quad\hat{X}^2+\hat{Z}^2\to\infty. \tag{5.10}$$

Guided by this we write

$$\hat{A}=(\lambda^2\hat{X}^2+\hat{Z}^2+\alpha_0^2)^{\frac{1}{2}}-\frac{\hat{\gamma}(\hat{Z})+\alpha_0^2}{2(\lambda^2\hat{X}^2+\hat{Z}^2+\alpha_0^2)^{\frac{1}{2}}}+\tilde{A}, \tag{5.11}$$

where now we have $\tilde{A}\to 0$ as $\hat{X}^2+\hat{Z}^2\to\infty$. We have introduced the (artificial) constant α_0 into the problem in order to ensure boundedness as $\hat{X}^2+\hat{Z}^2\to 0$. (This is mirrored in $(\hat{k},\hat{l})$-space by appropriate decay as $\hat{k}^2+\hat{l}^2\to\infty$; setting $\alpha_0=0$ would cause difficulties with the transform in this limit.) α_0 may take on any real value, and is thus a parameter entirely of our choice, the exact solution for $\hat{A}$ being completely independent of α_0.

Substituting (5.11) into (5.9) yields

$$\left\{\frac{[\hat{\gamma}(\hat{Z})+\alpha_0^2]^2}{4r^2}+2\tilde{A}r+\tilde{A}^2-\frac{\tilde{A}[\hat{\gamma}(\hat{Z})+\alpha_0^2]}{r}\right\}^{**}=-(\mathrm{i}\hat{k})^{\frac{1}{2}}(\hat{k}^2+\hat{l}^2)^{\frac{1}{2}}\left\{r-\frac{\hat{\gamma}(\hat{Z})+\alpha_0^2}{2r}+\tilde{A}\right\}^{**}. \tag{5.12}$$

Here, for convenience, we have written

$$r=(\lambda^2\hat{X}^2+\hat{Z}^2+\alpha_0^2)^{\frac{1}{2}}. \tag{5.13}$$

Unfortunately (5.12) is still not quite suitable for numerical treatment (because of difficulties with the second term on the left-hand side of (5.12) as $\hat{X}^2+\hat{Z}^2\to\infty$). This may be rectified, however, by writing

$$\tilde{A}=A_0+B, \tag{5.14}$$

where

$$[2A_0 r]^{**}=-(\mathrm{i}\hat{k})^{\frac{1}{2}}(\hat{k}^2+\hat{l}^2)^{\frac{1}{2}}\left\{r-\frac{[\hat{\gamma}(\hat{Z})+\alpha_0^2]}{2r}\right\}^{**}. \tag{5.15}$$

Details of the evaluation of A_0 are given in the Appendix, but now we may regard A_0 as a known function of $\hat{X}$ and $\hat{Z}$ (or A_0^{**} as a known function of $\hat{k}$ and $\hat{l}$), and B the function to be determined.

Equation (5.12) may now instead be written

$$\left\{\frac{[\hat{\gamma}(\hat{Z})+\alpha_0^2]^2}{4r^2}+2Br-[\gamma(Z)+\alpha_0^2]\left[\frac{A_0}{r}+\frac{B}{r}\right]+A_0^2+2A_0B+B^2\right\}^{**}$$
$$=-(\mathrm{i}\hat{k})^{\frac{1}{2}}(\hat{k}^2+\hat{l}^2)^{\frac{1}{2}}(A_0+B)^{**}. \tag{5.16}$$

Equation (5.16) is cast in $(\hat{k},\hat{l})$-space; however, although its right-hand side is most simply evaluated in its present form in Fourier space, the left-hand side is best evaluated in physical space. Consequently we choose to adopt a solution procedure that exploits the favourable aspects of both spaces. More specifically, the technique is as follows.

For a given $\hat{\gamma}(\hat{Z})$, A_0, then A_0^{**} and the inverse of $(\mathrm{i}\hat{k})^{\frac{1}{2}}(\hat{k}^2+\hat{l}^2)^{\frac{1}{2}}A_0^{**}$ are all evaluated (see Appendix for details). Then some guessed $B(\hat{X},\hat{Z})$ (on a discrete set of $\hat{X}$- and $\hat{Z}$-points) is transformed into $(\hat{k},\hat{l})$-space to yield $B^{**}(\hat{k},\hat{l})$. This is achieved using the fast Fourier transform (FFT) technique of Cooley & Tukey (1965). The term $(\mathrm{i}\hat{k})^{\frac{1}{2}}(\hat{k}^2+\hat{l}^2)^{\frac{1}{2}}B^{**}$ is then constructed, and transformed back to physical space (again by means of the FFT technique). This yields an estimate for the right-hand side of (5.16) on the $(\hat{X},\hat{Z})$-grid, and provides a means of obtaining a new estimate for $B(\hat{X},\hat{Z})$. A number of different schemes were utilized for this, but the most reliable, generally, (although not always the scheme that gave the most rapid convergence) was to write (5.16) at each $(\hat{X},\hat{Z})$-location as

$$B = R-\alpha_1 B^2, \tag{5.17}$$

and to use this to provide a new estimate for B, treating the right-hand side of this equation as known (some under-relaxation was applied if necessary). In certain regions of parameter space, this iteration procedure was modified slightly by using (5.17) at all $(\hat{X},\hat{Z})$-stations, except at one (prescribed) station, $(\hat{X}_0,\hat{Z}_0)$ say $B(\hat{X}_0,\hat{Z}_0)$ was prescribed and $\hat{\gamma}(\hat{Z}_0)$ was treated as the unknown (a similar tactic was followed in I). The process was repeated until the maximum change to the solution at any of the (X,Z)-points fell below some predetermined tolerance (10^{-5}). Since we are concerned with flows that are symmetric with respect to $Z=0$, we need only consider $Z\leqslant 0$. Further, notice that if we use a grid size in $\hat{X}$ of $\Delta\hat{X}$, with N_X points, the grid in $\hat{k}$-space is given by

$$\Delta\hat{k} = 2\pi/N_X\,\Delta\hat{X}. \tag{5.18}$$

This relationship arises through the use of the FFT. A similar relationship applies in the crossflow direction,

$$\Delta\hat{l} = 2\pi/N_Z\,\Delta\hat{Z}, \tag{5.19}$$

where $\Delta\hat{Z}$ is the grid size in the $\hat{Z}$-direction, N_Z the number of grid points, and $\Delta\hat{l}$ the grid size in $\hat{l}$-space.

In the following section we go on to describe a number of results.

6. Results and discussion

As a check of the general numerical technique, the two-dimensional case as considered in I was recomputed, using basically the same technique as described in the previous section. This involved solving (5.9) with $\hat{Z}=0$, $\hat{l}=0$, $\lambda=1$, $\hat{\gamma}(\hat{Z})=\Gamma$ (a constant), with just a single Fourier Transform (in the $\hat{X}$-direction). Additionally, the particular details, given in the Appendix, are rather different, although the overall scheme was similar.

The two-dimensional case was computed with $N_X=64$, $\Delta\hat{X}=0.317$, and $\alpha_0=3$; the variation of $\hat{A}(\hat{X}=0)$ with Γ is shown in figure 1. The value of A here differs by a multiplicative factor $\pi^{\frac{1}{2}}$ from that of I, and the value of Γ here by a multiplicative factor $\pi^{\frac{2}{5}}$ from that of I (on account of the slightly different normalization used); to facilitate comparison, figure 1 also indicates the values corresponding to the normalization of I (these are denoted by a subscript I). The present results reproduce

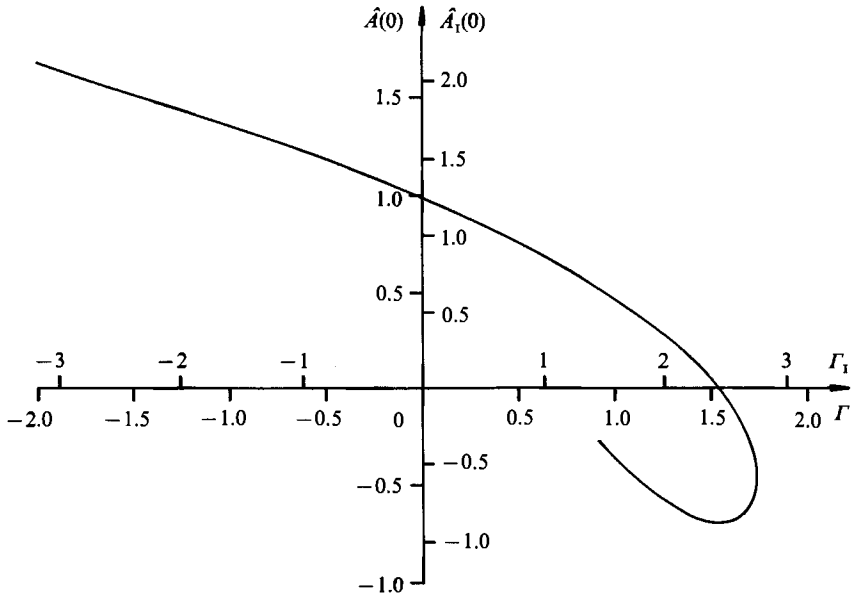

FIGURE 1. Variation of $\hat{A}(0)$ with Γ (two-dimensional case). $\hat{A}_I, \hat{\Gamma}_I$ denote values using the normalization of I.

those of I, to within graphical accuracy. The non-uniqueness of the solution over a range of Γ, together with the non-existence of a solution for $\Gamma \geqslant 1.74$, is immediately apparent. On the 'lower branch' of the curve, computations became progressively more awkward as Γ was reduced, even using the alternative procedure where Γ itself is determined during the course of the iteration (although no really exhaustive attempt was made to extend these results further, the accuracy of the scheme having been confirmed).

We now consider a number of results for the three-dimensional case. To be specific, we shall focus attention on functions $\hat{\gamma}(\hat{Z})$ of the class

$$\hat{\gamma}(\hat{Z}) = \Gamma \mathrm{e}^{-\hat{Z}^2}, \tag{6.1}$$

and seek to determine the variation of solutions with Γ. (Note that even though this choice makes $\hat{\gamma}(\hat{Z}) \to 0$ as $\hat{Z} \to \infty$, the results will nonetheless be fully three-dimensional, as can be seen by the form of the far-field conditions (4.19).)

Variations of $\hat{A}(\hat{X}, \hat{Z})$ (at selected $(\hat{X}, \hat{Z})$-stations) are shown in figure 2. These results were determined with the grid $N_Z = N_X = 64$, $\Delta\hat{X} = \Delta\hat{Z} = 0.317$, and $\alpha_0 = 3$, for the particular case $\lambda = 1$. These distributions are qualitatively similar to those obtained for the two-dimensional case, although the range of Γ for which solutions exist is much increased. To assess the effect of numerical grid changes, figure 3 shows results for $\hat{A}(\hat{X} = 0, \hat{Z} = 0)$, obtained using: $\alpha_0 = 3, N_X = N_Z = 32, \Delta\hat{X} = \Delta\hat{Z} = 0.645$; $\alpha_0 = 2$, $N_X = N_Z = 64$, $\Delta\hat{X} = \Delta Z = 0.317$; and $\alpha_0 = 3$, $N_X = N_Z = 16$, $\Delta\hat{X} = \Delta\hat{Z} = 0.667$.

It is heartening that there appears to be no difference (to within graphical accuracy) between the $\alpha_0 = 3$ and corresponding $\alpha_0 = 2$ results (indeed the computation was also carried out with $\alpha_0 = 2$, $N_X = N_Z = 32$, $\Delta\hat{X} = \Delta\hat{Z} = 0.645$, and this too gave results indistinguishable on the graphical scale used from the corresponding $\alpha_0 = 3$ calculation). On the whole the computations agree very well, although the most prominent discrepancy occurs in the 'nose' region of the curve, as

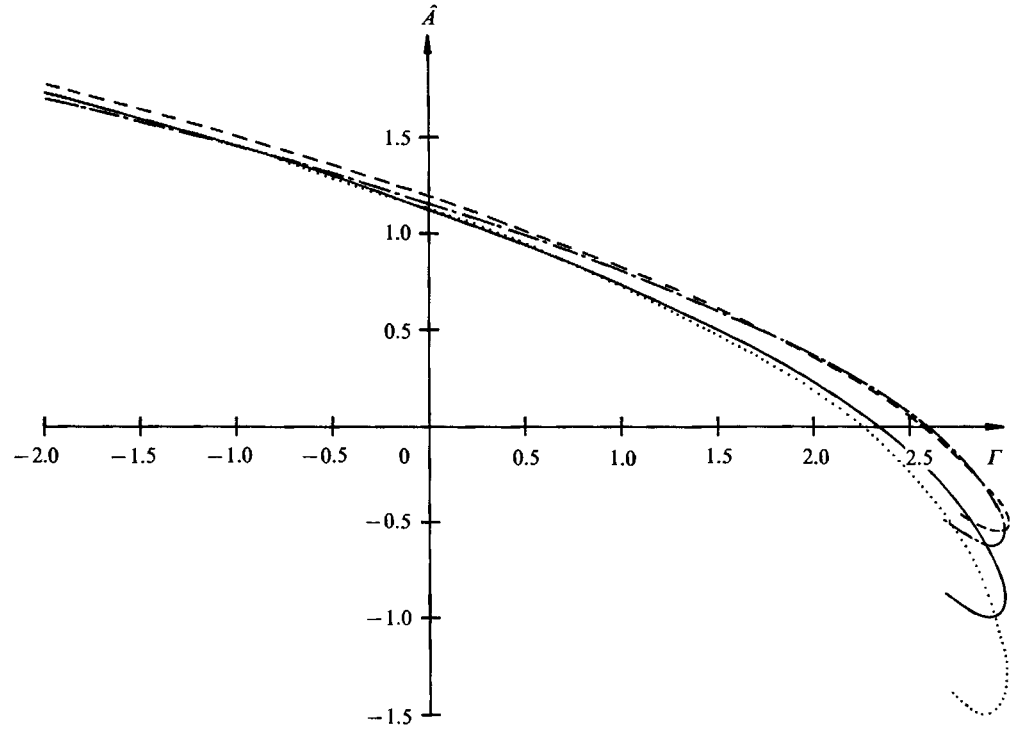

FIGURE 2. Variations of $\hat{A}(\hat{X},\hat{Z})$ at selected $(\hat{X},\hat{Z})$-stations, $\hat{\gamma}(\hat{Z}) = \Gamma e^{-\hat{z}^2}$, $N_X = N_Z = 64$, $\Delta\hat{X} = \Delta\hat{Z} = 0.317$, $\alpha_0 = 3$, $\lambda = 1$. ——, $\hat{X} = \hat{Z} = 0$; – – –, $\hat{X} = -0.3175$, $\hat{Z} = 0$; ....., $\hat{X} = 0.3175$, $\hat{Z} = 0$; —·—, $\hat{X} = 0$, $\hat{Z} = -0.3175$.

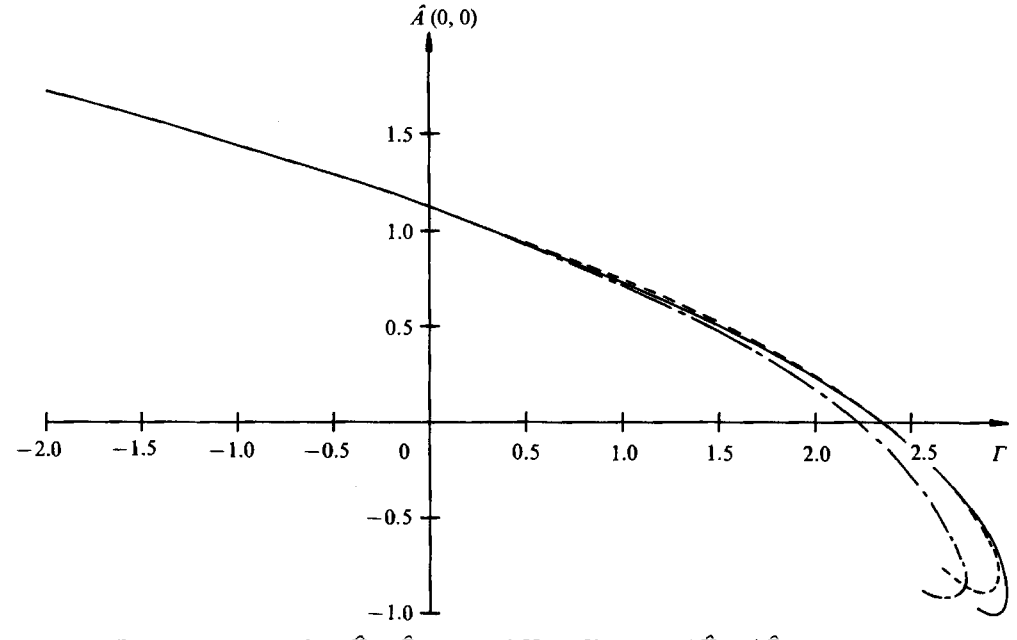

FIGURE 3. Details as above, but $\hat{X} = \hat{Z} = 0$; and $N_X = N_X = 64$, $\Delta\hat{X} = \Delta\hat{Z} = 0.317$, $\alpha_0 = 2$ (——); $N_X = N_Z = 32$, $\Delta\hat{X} = \Delta\hat{Z} = 0.645$, $\alpha_0 = 3$ (– – – –); $N_X = N_Z = 16$, $\Delta\hat{X} = \Delta\hat{Z} = 0.667$, $\alpha_0 = 3$ (— · —).

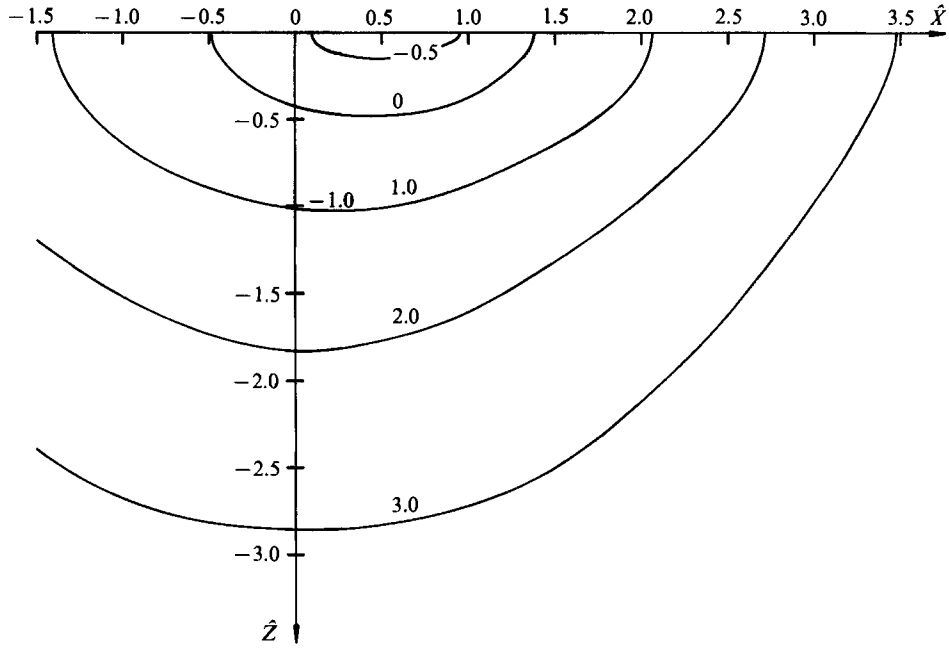

FIGURE 4. Contours for constant $\hat{A}(\hat{X},\hat{Z})$, $\hat{\gamma}(\hat{Z}) = 2.803\,103\,\mathrm{e}^{-\hat{Z}^2}$, $\lambda = 1$, upper-branch solution.

may be anticipated, although elsewhere the agreement is to within the accuracy of the figure. The computations on the 'lower branch' became progressively more difficult as Γ was reduced (a typical computation on the finest, most extensive grid taking of the order of ten minutes on a Cray XMP), and so the curves are not extended as far as the corresponding two-dimensional case (figure 1).

Figure 4 shows the contours of constant $\hat{A}(\hat{X},\hat{Z})$ for $\Gamma = 2.803\,103$ (upper branch) and for comparison figure 5 shows the contours for the same value of Γ, but corresponding to the lower branch (both sets of results were obtained using the same grid as used for figure 2). Since $\hat{A}(\hat{X},\hat{Z})$ is proportional to the streamwise wall shear, negative $\hat{A}(\hat{X},\hat{Z})$ implies reversed flow. Comparing these two figures reveals the lower branch to involve a much larger region of reversed flow. Indeed, as the lower branch is followed, with Γ reducing, the region of reversed flow is expected to increase without bound (a feature observed in previous two-dimensional studies). As $\hat{X}^2+\hat{Z}^2$ increases, the contours became progressively more circular in both cases.

Figure 6 shows the variation of $\hat{A}(\hat{X}=0,\hat{Z}=0)$ with Γ for the case $\lambda = 2$ (obtained using the grid $N_X = N_Z = 64$, $\Delta\hat{X} = \Delta\hat{Z} = 0.317$, and $\alpha_0 = 3$). This case corresponds to a basic flow with a rather stronger streamwise flow near the wall compared with the crossflow. In this case the range of Γ over which the solution exists is increased over the $\lambda = 1$ results, as in the range of $\hat{A}(0,0)$. Figure 7 shows contours of constant $\hat{A}(\hat{X},\hat{Z})$ for $\Gamma = 5.342\,597$ (lower branch). The contours as $\hat{X}^2+\hat{Z}^2 \to \infty$ in this case will no longer approach the circular form of $\lambda = 1$, but rather will tend to ellipses.

These results clearly illustrate the occurrence of fully three-dimensional solutions involving below-marginal skin friction. The basic solution technique introduced here, involving the usage of a pseudospectral method, could fairly easily be extended to other classes of flow, for example flows away from lines of symmetry, supersonic three-dimensional flows or flows where $U_0'(0)$ and $W_1'(0)$ do not vanish simultaneously (such as that studied in II). However the particular details required in obtaining

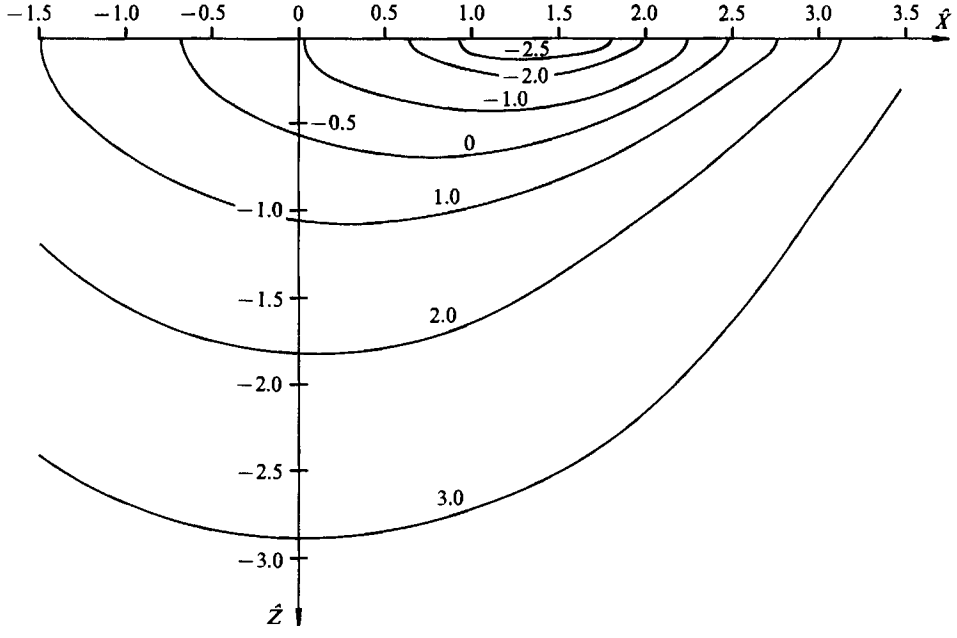

FIGURE 5. Contours for constant $\hat{A}(\hat{X}, \hat{Z})$, $\hat{\gamma}(\hat{Z}) = 2.803\,103\,\mathrm{e}^{-\hat{Z}^3}$, lower-branch solution.

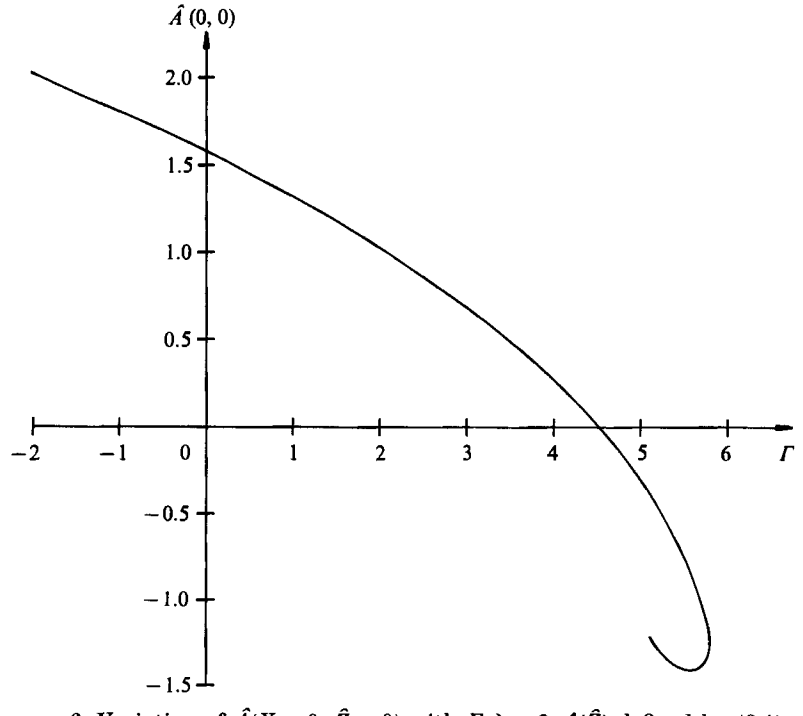

FIGURE 6. Variation of $\hat{A}(X = 0, \hat{Z} = 0)$ with $\Gamma, \lambda = 2$, $\hat{\gamma}(\hat{Z})$ defined by (6.1).

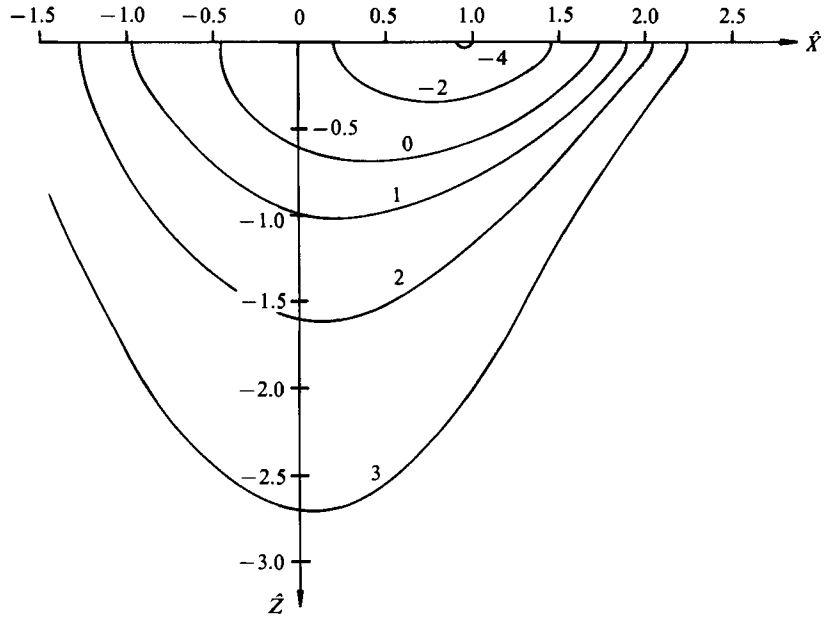

FIGURE 7. Contours for constant $\hat{A}(\hat{X},\hat{Z})$, $\hat{\gamma}(\hat{Z}) = 5.342597\,\mathrm{e}^{-\hat{Z}^2}$, $\lambda = 2$, lower-branch solution.

a well-behaved 'perturbation' solution to compute (cf. the Appendix) would necessarily have to be modified. Further, and importantly, the theory presented here is not subject to the limitations imposed as a result of the essentially two-dimensional interaction condition employed in II.

It is worth making a few final comments regarding the choice and determination of the function $\hat{\gamma}(\hat{Z})$. In this paper $\hat{\gamma}(\hat{Z})$ represents a quite natural extension of the constant Γ found in the two-dimensional work of I (and $\Gamma_{\pm}$ in II). In I, Γ was interpreted as being proportional to the excess of the angle of incidence (or camber) over the critical value. As described in II, the interpretation of the two related constants $\Gamma_{\pm}$ occurring in that study is less obvious. In the present work, we may interpret $\hat{\gamma}(\hat{Z})$ as being a measure of the excess angle over the critical centreline angle; in the present context the local angle can depend on spanwise location, and so this excess will in general be a function of lateral position, which from a physical point of view can be regarded as a spanwise (i.e. $\hat{Z}$) variation of body surface curvature and/or of streamwise conditions (we must however restrict spanwise variations to be on a scale $z = O(\delta)$ or longer).

Our particular choice of $\hat{\gamma}(\hat{Z})$, namely (6.1), leads necessarily to a model problem; however because of the qualitative similarity between the results for this particular choice of $\hat{\gamma}(\hat{Z})$ and those found in I and II, we fully expect the present three-dimensional results to give a good indication of the qualitative feature of general flows of this class. Since $\hat{\gamma}(\hat{Z})$ represents an 'excess' over the critical state, by its nature it controls the amount of interaction in the problem (see also the remarks towards the end of §4 regarding this point). Hence it is not directly deducible from 'non-interacting' calculations such as those of Cebeci & Su (1988). (The constant Γ found in I is also not directly obtainable from 'non-interacting' calculations.)

The author wishes to thank Professor O. R. Burggraf for encouragement and many useful discussions relating to this work. Computations were carried out at the Ohio Supercomputer Center, the University of Manchester Regional Computer Centre (with computer time provided under SERC Grant No. GR/E/25702) and at NASA Lewis Research Center (whilst the author was visiting under the ICOMP program).

Appendix. The evaluation of $\hat{A}_0$ and $\hat{A}_0^{**}$

Since certain of the components in the evaluation of $\hat{A}_0$ are unbounded as $\hat{X}^2+\hat{Z}^2\to\infty$ (and this is reflected by singularities as $\hat{k}^2+\hat{l}^2\to 0$ in Fourier space), a certain amount of analytic work is necessary, prior to any numerics. Fortunately, the inclusion of the α_0 term (see (5.11)) ensures decay in $(\hat{k},\hat{l})$-space as $\hat{k}^2+\hat{l}^2\to\infty$, and so this limit requires no special attention.

By (5.15) we have

$$(r\hat{A}_0)^{**} = -\tfrac{1}{2}(\mathrm{i}\hat{k})^{\frac{1}{2}}(\hat{k}^2+\hat{l}^2)^{\frac{1}{2}}\left\{r-\frac{[\hat{\gamma}(\hat{Z})+\alpha_0^2]}{2r}\right\}^{**}. \tag{A 1}$$

It is straightforward to show that

$$r^{**} = -2\pi(\hat{k}^2+\hat{l}^2\lambda^2)^{-\frac{3}{2}}\lambda^2\left[1+\frac{\alpha_0(\hat{k}^2+\lambda^2\hat{l}^2)^{\frac{1}{2}}}{l}\right]\exp\left[-\frac{\alpha_0}{\lambda}(\hat{k}^2+\hat{l}^2\lambda^2)^{\frac{1}{2}}\right] \tag{A 2}$$

(assuming $\alpha_0>0$).

The quantity $r^{**}(\mathrm{i}\hat{k})^{\frac{1}{2}}(\hat{k}^2+\hat{l}^2)^{\frac{1}{2}}$ is transformed back to $(\hat{X},\hat{Z})$-space by the integral

$$-\frac{4\lambda^2}{\pi}\int_0^\infty\int_0^{\frac{1}{2}\pi}\frac{(\cos\phi)^{\frac{1}{2}}}{\Phi^3}\exp\left[-\frac{\alpha_0}{\lambda}\hat{\rho}^2\Phi\right]\left(1+\alpha_0\frac{\hat{\rho}^2}{\lambda}\Phi\right)\cos(\hat{\rho}^2\cos\phi\hat{X} + \tfrac{1}{4}\pi)\cos(\hat{\rho}^2\sin\phi\hat{Z})\,\mathrm{d}\hat{\rho}\,\mathrm{d}\phi, \tag{A 3}$$

where

$$\Phi = [\cos^2\phi+\lambda^2\sin^2\phi]^{\frac{1}{2}}. \tag{A 4}$$

Here the Fourier variables $\hat{k},\hat{l}$ have been transformed to Fourier polar variables $\bar{\rho},\phi$, and then the radial variable $\hat{\rho}$ is introduced by $\bar{\rho}=\hat{\rho}^2$. The result (A 3) is a fairly well-behaved integral, which is readily amenable to numerical quadrature (the weak square-root singularity at $\phi=\frac{1}{2}\pi$ was not found to cause any difficulties).

The $\alpha_0^2/2r$-term in (A 1) was treated in much the same way as above, using the result

$$\left(\frac{1}{r}\right)^{**} = 2\pi(\hat{k}^2+\lambda^2\hat{l}^2)^{-\frac{1}{2}}\exp\left[-\frac{\alpha_0}{\lambda}(\hat{k}^2+\hat{l}^2\lambda^2)^{\frac{1}{2}}\right]. \tag{A 5}$$

The remaining term was evaluated rather more numerically. We have

$$\left[\frac{\hat{\gamma}(\hat{Z})}{2r}\right]^{**} = 2\int_0^\infty\hat{\gamma}(\hat{Z})\cos\hat{l}\hat{Z}K_0\left[\frac{\hat{k}}{\lambda}(\hat{Z}^2+\alpha_0^2)^{\frac{1}{2}}\right]\mathrm{d}\hat{Z} \tag{A 6}$$

(having carried out the $\hat{X}$-transform). Here $K_0(\chi)$ denotes the modified Bessel function of order zero, argument χ. The $\hat{Z}$-integration generally requires a numerical treatment (depending on the particular form for $\hat{\gamma}(\hat{Z})$). Once evaluated, the quantity $(\mathrm{i}\hat{k})^{\frac{1}{2}}(\hat{k}^2+\hat{l}^2)^{\frac{1}{2}}\{\hat{\gamma}(\hat{Z})/2r\}^{**}$ was then transformed to $(\hat{X},\hat{Z})$ numerically, completing the

determination of A_0. A_0^{**} was then evaluated without any special numerical treatment, $(i\hat{k})^{\frac{1}{2}}(\hat{k}^2+\hat{l}^2)^{\frac{1}{2}}A_0^{**}$ was constructed, and then transformed back to (X,Z)-space (again, with no special treatment), thus completing the preliminary computation, prior to the iteration commencing.

REFERENCES

BODONYI, R. J. & DUCK, P. W. 1988 A numerical method for treating strongly interactive three-dimensional viscous–inviscid flows. *Computers Fluids* **16**, 279.

BROWN, S. N. 1985 Marginal separation of a three-dimensional boundary layer on a line of symmetry. *J. Fluid Mech.* **158**, 95.

BROWN, S. N. & STEWARTSON, K. 1983 On an integral equation of marginal separation. *SIAM J. Appl. Maths* **43**, 1119.

CEBECI, T., KHATTAB, A. K. & STEWARTSON, K. 1980 On nose separation. *J. Fluid Mech.* **97**, 435.

CEBECI, T. & SU, W. 1988 Separation of three-dimensional laminar boundary layers on a prolate spheroid. *J. Fluid Mech.* **191**, 47.

COOLEY, J. W. & TUKEY, J. W. 1965 An algorithm for the machine computation of complex Fourier series. *Maths Comp.* **19**, 297.

DUCK, P. W. & BURGGRAF, O. R. 1986 Spectral solutions for three-dimensional triple-deck flow over surface topography. *J. Fluid Mech.* **162**, 1.

FORNBERG, B. 1980 A numerical study of steady viscous flow past a circular cylinder. *J. Fluid Mech.* **98**, 819.

FORNBERG, B. 1985 Steady viscous flow past a circular cylinder up to a Reynolds number 600. *J. Comp. Phys.* **61**, 297.

GOLDSTEIN, S. 1948 On laminar boundary layer flow near a point of separation. *Q. J. Mech. Appl. Maths* **1**, 43.

LIGHTHILL, M. J. 1963 Boundary layer theory. In *Laminar Boundary Layers* (ed. L. Rosenhead), chap. II. Oxford University Press.

PEREGRINE, D. H. 1985 A note on the steady high-Reynolds-number flow about a circular cylinder. *J. Fluid Mech.* **157**, 493.

SMITH, F. T. 1979 Laminar flow of a incompressible fluid past a bluff body; the separation, reattachment, eddy properties and drag. *J. Fluid Mech.* **92**, 171.

SMITH, F. T. 1982 Concerning dynamic stall. *Aero Q.* **33**, 331.

SMITH, F. T. 1983 Properties, and a finite-difference approach, for three-dimensional interactive boundary layers. *UTRC Rep.* 83-46. United Technical Res. Cent. East Hertford, CN.

SMITH, F. T. 1985 A structure for laminar flow past a bluff body at high Reynolds number. *J. Fluid Mech.* **155**, 175.

SMITH, F. T., SYKES, R. I. & BRIGHTON, P. W. M. 1977 A two-dimensional boundary layer encountering a three-dimensional obstacle. *J. Fluid Mech.* **83**, 163.

STEWARTSON, K. 1970 Is the singularity at separation removable? *J. Fluid Mech.* **44**, 347.

STEWARTSON, K., SMITH, F. T. & KAUPS, K. 1982 Marginal separation. *Stud. Appl. Maths* **67**, 45.